Climate nonlinearities: selection, uncertainty, projections, & damages

B. B. Cael[1,*], G. L. Britten[2], F. Mir Calafat[1], J. Bloch-Johnson[3], D. Stainforth[4], & P. Goodwin[5]

1. National Oceanography Centre, Southampton, UK. 2. Massachusetts Institute of Technology, Cambridge, USA. 3. National Centre for Atmospheric Science, Reading, UK. 4. London School of Economics, UK. 5. University of Southampton, UK.

Email addresses: cael@noc.ac.uk, gregleebritten@gmail.com, francisco.calafat@noc.ac.uk, j.bloch-johnson@reading.ac.uk, d.a.stainforth@lse.ac.uk, p.a.goodwin@soton.ac.uk

This paper is a non-peer reviewed preprint submitted to EarthArXiv. This paper is in review at *Environmental Research Letters*.

*Corresponding author.

Author Contributions: Cael lead all aspects of this work, with assistance from all other authors in methodology, interpretation, and writing.

Article Type: Letter

Keywords: Climate change | Bayesian statistics | Energy balance model | Integrated assessment model | Structural uncertainty | Feedback temperature dependence

Data Availability: All data used here are publicly available at the sources cited in the text. Code will be made available and given a doi via Github and Zenodo if this manuscript is accepted for publication.

Conflicts: The authors have no competing interests to declare.

Abstract: Climate projections are highly uncertain; this uncertainty is costly and impedes progress on climate policy. This uncertainty is primarily parametric (what numbers do we plug into our equations?) and structural (what equations do we use in the first place?). The former is straightforward to characterise in principle, though may be computationally intensive for complex climate models. The latter is more challenging to characterise and is therefore often ignored. We developed a Bayesian approach to quantify structural uncertainty in climate projections, using the idealised energy-balance model representations of climate physics that underpin many economists' integrated assessment models (and therefore their policy recommendations). We define a model selection parameter, which switches on one of a suite of proposed climate nonlinearities and multidecadal climate feedbacks. We find that a temperature-dependent climate feedback is most consistent with global mean surface temperature observations, but that the sign of the temperature-dependence is opposite of what Earth system models suggest. This discrepancy is likely due to the assumption that the recent pattern effect can be represented as a temperature dependence. Moreover, the most likely model is less probable than the rest of the models combined, indicating that structural uncertainty is important for climate projections. Indeed, under shared socioeconomic pathways similar to current emissions reductions targets, structural uncertainty dwarfs parametric uncertainty in temperature. Consequently, structural uncertainty dominates overall non-socioeconomic uncertainty in economic projections of climate change damages, as estimated from a simple temperature-to-damages calculation. These results indicate that considering structural uncertainty is crucial for integrated assessment models in particular, and for climate projections in general.

Introduction

Anthropogenic emissions increase the concentration of greenhouse gases in the atmosphere, resulting in a radiative forcing F [W/m^2] on the Earth system. How this forcing will affect Earth's global mean surface temperature T [°C] has been highly uncertain [6] and will likely continue to be so. This uncertainty hampers the design and implementation of appropriate climate planning and policies, which costs on the order of trillions of dollars [14]. A core objective of modern Earth system research is thus to improve climate change projections. Earth's climate system is extraordinarily complex and mulitfaceted, meaning there are myriad sources of uncertainty. On the one hand, very complex Earth system models (ESMs), which attempt to represent as many of these processes as possible, are too computationally expensive to gauge how uncertainties propagate into uncertainty in T or other properties of interest. Thus the Intergovernmental Panel on Climate Change largely relies upon a heuristic characterisation of uncertainties [17]. On the other hand, simpler models of climate physics, such as the energy balance models (EBMs) used within the integrated assessment models (IAMs) of economists [4], or efficient reduced-complexity ESMs [10], can produce large ensembles of simulations, intended to characterise this uncertainty. While ESMs are typically the core tool for of climate science projections such as in [17], EBMs are used to emulate ESMs, to explore alternative scenarios, assess parametric uncertainty, constrain with observations, and to represent climate physics within climate economics; thus both model frameworks are fundamentally important in guiding climate policy.

Climate model ensembles tend to characterise *parametric* uncertainty – uncertainty associated with the numerical values of parameters used in these models. A second type of uncertainty, which is generally overlooked because it is more difficult to quantify, is *structural* uncertainty – what equations we use for these models in the first place. Models along the entire axis of complexity are subject to structural uncertainty for different reasons; ESMs have many equations, some of which are derived from first principles and thus known with certainty but many of which are not, while EBMs and IAMs have fewer approximating equations and thus may be less adequate for representing complex earth system processes. Therefore, structural uncertainty may increase or decrease with model complexity, and may either dwarf or be negligible compared to parametric uncertainty; this is unknown because of the lack of quantitative characterisation of structural uncertainty in climate models across the full axis of complexity. While quantifying structural uncertainty for ESMs is no less challenging due to computational limitations than parametric uncertainty, EBMs and IAMs for which structural uncertainty has been neglected do not suffer this limitation.

Here we present a means to quantify structural uncertainty in a simple EBM used by several IAMs, though our approach is generalisable to climate models with additional complexity. We show that structural uncertainty is much larger than parametric uncertainty for projections of T, and consequently for calculations of damages due to climate change. (We note that economic models have additional uncertainties; here we are only interested in how physical uncertainty propagates into uncertainty in economic calculations.) This dominance of structural uncertainty occurs despite a particular model structure being the most consistent with observations. These results underscore that physical structural uncertainty is substantial in climate economics calculations, and in climate projections in general. They also imply that reported uncertainties of such projections may be appreciably underestimated, as is often the case with complex physical phenomena. [12].

Materials and Methods

Note that an extended description of the methods is given in the supplemental material (SM). We are interested in making projections of Earth's global mean surface temperature T due to radiative forcing F resulting from greenhouse gases, aerosols, ozone precursors, land use change, and other anthropogenic influences. A computational Bayesian approach to this problem essentially 1) specifies a model that represents this process, 2) specifies prior distributions for the parameters of this model, 3) draws samples from these priors, 4) computes the relative likelihood of these draws according to how well or poorly they correspond to observations of this process, 5) weighs these samples according to this likelihood, and 6) uses this weighted ensemble (i.e. the posterior distribution) of samples to project into the future probabilistically. The model that we start from is the standard linear energy balance model used in IAMs like PAGE and FUND [4]:

$$c\dot{T} = F - \lambda T$$

where c is the heat capacity of the surface layer represented by T, the dot represents the first time derivative, and λ is the climate feedback parameter. This parameter includes both upwards and downwards energy fluxes out of the layer to which T corresponds (SM), which is more commonly referred to as the climate resistance (given the symbol ρ and is equal to the sum of the climate feedback λ and the ocean heat uptake efficiency κ) in the climate physics literature e.g. [11]. However, we retain the symbol λ and terminology of climate feedback to be consistent with the economics literature. Note this also changes the interpretation of feedback temperature dependence somewhat in the λ_T case below.

We then use this model, a multidecadal feedback λ_s [8], or one of four Taylor-expansion-based nonlinearities (a F-/T-dependent c/λ) [3] depending on the value of a model selection parameter μ. Formally this is written

$$\begin{aligned} c(1+\nu\mathbb{1}_{\mu=2}T+\nu\mathbb{1}_{\mu=3}F)\dot{T} = \\ F+\lambda(1+\nu\mathbb{1}_{\mu=4}T+\nu\mathbb{1}_{\mu=5}F)T \\ +\mathbb{1}_{\mu=6}\lambda_s\int_{-\infty}^{0}\frac{1}{\tau}T(t')e^{t'/\tau}\,dt' \end{aligned}$$

where ν is the amplitude of the nonlinearity selected by μ, and $\mathbb{1}$ is an indicator function. We also explored additional model structures and dropped them because they were excluded by our analysis, either because they ultimately held negligible posterior mass or because their corresponding parameters were constrained to be small enough that they reduced to other model types included in the above equation (see SM). Prior distributions for each of these parameters are then specified based on knowledge from fundamental physical principles, Earth system models, similar Bayesian climate modelling approaches, observational products other than the one used to construct the likelihood function, and to construct the problem in a fashion well-suited to answering the scientific question at hand. Most notably, with respect to the last of these, we specify a uniform prior for μ so that all six model formulations (linear, $\lambda_{T,F}$, $c_{T,F}$, and λ_s) are initially considered equally plausible. Note that one may also think of this equivalently as each model described in the SM, where μ is set to a particular integer value and all, or all but one, of the terms multiplied by the indicator function in the equation above is thereby cancelled out, is fit to the observations separately. Then, the grand ensemble is built from a combination of each individual model ensemble, weighted by its respective posterior.

We then draw many samples from these priors and from an ensemble of radiative forcing time series [23, 17] to generate many model temperature time series, and evaluate how well each time series captures the observed time series [18] from 1850-2020 to assign each sample a likelihood. We then force this ensemble with future projections of radiative forcing under different emissions scenarios [19] to generate probabilistic projections. We then use the a damage and discounting function from [5] to translate these temperature projections into economic damages due to climate change.

When restricting to the ensembles for individual μ values, these projections capture parametric uncertainty for each model structure. The remaining spread in the projections across all μ values is then due to structural uncertainty. We define a simple metric for the importance of structural uncertainty:

$$u(X) = \frac{IQR(X)}{IQR_p(X)} - 1$$

where $IQR(X)$ is the interquartile range of the multi-model projection of the quantity X (e.g. T in 2100, or

total damages due to climate change), and $IQR_p(X)$ is the interquartile range of the projection of X by the preferred model structure, i.e. the one with the highest posterior μ mass. If $u(X)$ is close to zero, then either the preferred model structure holds nearly all of the posterior probability, or the differences between model structures do not make an appreciable difference to the projection. If $u > 1$, however, then the uncertainty in X due to uncertainty in the model structure is greater than that due to the uncertainty in the preferred model's parameters (because the structural-plus-parametric uncertainty is more than double the parametric uncertainty).

Results and Discussion

Figure 1 shows the posterior for μ resulting from the analysis above. The temperature-dependent feedback model has more probability mass than the other models, with $p(\mu = 2) = 0.45$. Interestingly, the sign of λ_T (or equivalently ν conditional on $\mu = 2$) is well-constrained as positive, i.e. $p(\nu > 0|\mu = 2) = 0.98$. This is a dampening nonlinearity, i.e. the warmer the Earth gets, more radiative forcing is required to warm it, or equivalently the lower its climate sensitivity, which is the opposite of what is typically seen in Earth system models [3]. This dampening nonlinearity is likely due to a pattern effect, as warming in recent decades has been more focused in regions of tropical convection [9], where warming is more efficient at countering radiative forcing [1] [7]. Note that this pattern effect is likely to be a robust feature of the climate system; while ESMs currently struggle to reproduce the full amplitude of the observed pattern effect, the existence of a pattern effect analogous to observations is a robust feature of ESMs [8]. Given that this shift is unlikely to continue as warming continues [2], the temperature-dependent feedback model may be underestimating future warming. As both the magnitude and rate of change in warming are increasing over time, while the model expresses the magnitude of climate feedback as dependent on the magnitude of warming, the sign of the posterior for λ_T may also reflect any process that causes a lag in climate feedback response that is dependent on the rate of change in warming. Either option could be due to a delayed change in the pattern of surface warming. Further analysis accounting for spatial variations is needed to distinguish between transient pattern effects and ongoing temperature dependence [21]. The methods proposed in this work would be of significant value in achieving more robust assessments of the structural uncertainty associated with these effects.

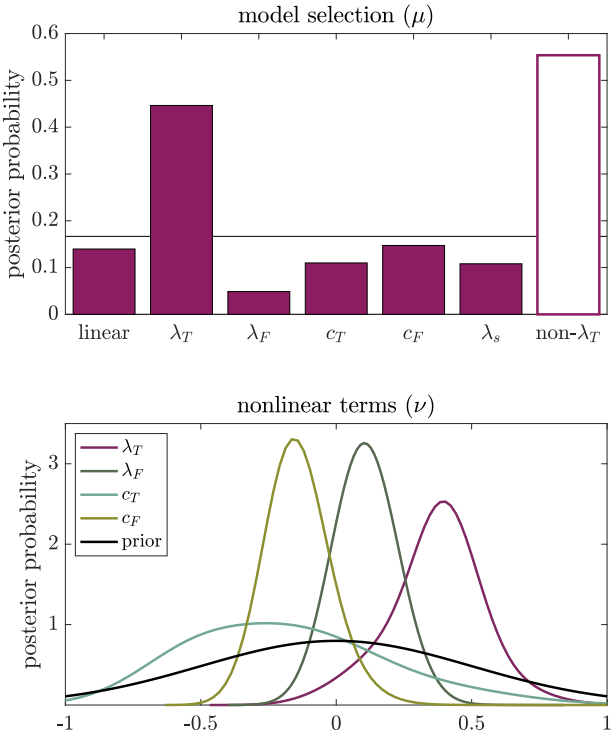

Figure 1. Top: Posterior mass for the model selection parameter μ. Non-λ_T refers to all models other than the temperature-dependent feedback model. Bottom: Posterior density for the nonlinear term ν in the four models with such a term.

Other posteriors are relatively informative; the posteriors for the other nonlinear terms are not sign-definite, while the posteriors for c, τ, and λ_s closely resemble their priors. One exception is that the lower-than-average time series of F are excluded from the posterior; $> 99\%$ of posterior probability is concentrated in ensemble members with an average of >2.1 W/m^2 over 1990-2020 (see Figure S1 in SM), corresponding to greater than the 64th percentile of the F time series ensemble (i.e. prior). This is in agreement with the finding in [10] that the most negative prior aerosol forcing values were excluded from the posterior (Fig. 3 therein). Additionally, λ is fairly well-constrained to be on the upper end of its prior for models without a nonlinear feedback term, or close to the modal value for λ for those with a nonlinear feedback term ($\mu = 4$ or 5; see Figure S2 in SM). These together suggest that the historical T observations are more consistent with a high-radiative forcing and corresponding high-feedback parameter set, which is consistent with the historical record yielding little information about climate sensitivity [22].

Despite there being a clear preferred model structure, 55% of the posterior mass is in the remaining models, i.e. $p(\mu \neq 2) = 0.55$. This strongly indicates an important role for structural uncertainty, especially given that the priors for the nonlinear terms in Figure 1 are fairly broad, which is also the case for λ_s. Figure 2 shows that indeed

structural uncertainty is dominant for temperature projections under shared socioeconomic pathway SSP4-6.0; in this case $u(T(2100)) = 2.0$ and $u(T(2300)) = 2.7$, indicating that structural uncertainty is far larger than parametric uncertainty. This is even more pronounced for SSP3-7.0 (see Figure S3 in SM), where $u(T(2100)) = 2.3$ and $u(T(2300)) = 4.1$. The multi-model median projection is also higher than the preferred-model-only projection; our focus here is on the uncertainty, however, especially given the discussion of the pattern effect above.

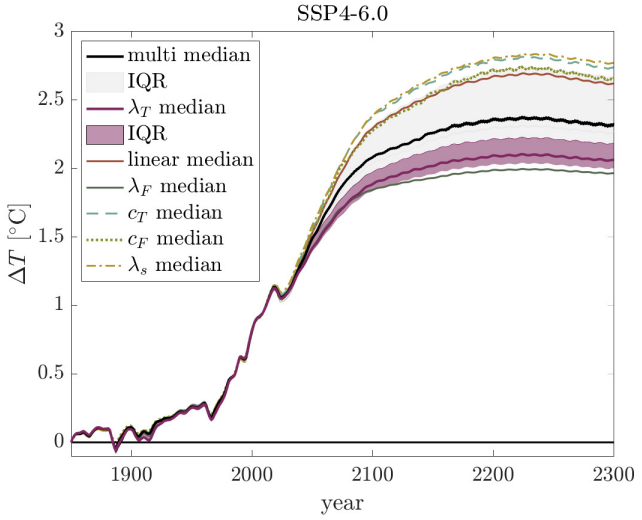

Figure 2. Projection of global mean surface temperature anomaly under the shared socioeconomic pathway SSP4-6.0. Lines denote the median projection of each model and of the multi-model ensemble. Purple (grey) shading denotes the interquartile range of projections for the temperature-dependent feedback model (multi-model ensemble).

The primacy of structural uncertainty in temperature projections propagates into economic damages resulting from climate change as well. Figure 3 shows the interquartile range of damage calculations using the approach and default assumptions from [5] for SSP4-6.0 and SSP3-7.0. In both cases, the dominance of structural uncertainty is even more pronounced than in temperature; u for damages is 2.9 for SSP4-6.0, and 4.6 for SSP3-7.0.

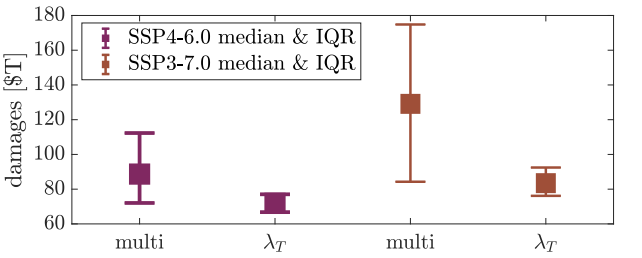

Figure 3. Median and interquartile range of damages projected under the socioeconomic pathways SSP4-6.0 and SSP3-7.0 for the temperature-dependent feedback model and the multi-model ensemble, in trillions of 2019 USD.

These results demonstrate the importance of characterising structural uncertainty for physical and economic projections of climate. While we have focused on arguably the simplest representation of climate physics, even this single-equation energy-balance model is used in a variety of applications for which structural uncertainty has real physical and economic consequences. Our approach to characterising structural uncertainty is equally applicable to more complex representations of climate physics, such as the model used in [10]; if such a model is computationally efficient enough to generate an ensemble that captures parametric uncertainty, one can also use model selection parameters for its different components (e.g. a parameter choosing between several representations of the ocean circulation) in the same fashion. Doing so will be critical for robust uncertainty characterisation of these models. Even the most complex Earth system models are subject to such structural uncertainty – possibly even more so as they involve so many parameterisations – though it is challenging to quantify either parametric or structural uncertainty with such computationally expensive models.

Reductions in structural uncertainty may be possible by incorporating known phenomena such as the El Niño Southern Oscillation or the pattern effect more explicitly than we have done here, or leveraging other observations such as that of ocean heat content [25]. However, not accounting for temperature fluctuations due to climate oscillations can lead to overfitting, i.e. overconfidence in the 'preferred' model structure, because stochastic interannual and decadal natural climate variability unduly influences the inference of parameters like λ; the same goes for neglecting autocorrelation of residuals because the information content in a time-series is overestimated. Similarly, paleo-records provide a wider dynamic range of radiative forcing and temperature than the observational record, suggesting an opportunity to constrain structural uncertainty further. However, these temperature and radiative forcing changes are being continuously revised for even the most recent period used for such purposes, the Last Glacial Maximum [20]. Scientists tend to substantially underestimate uncertainty in these contexts [12] and model selection is very sensitive to such changes and what paleo-periods are considered (Figures S4-S7). Paleo-observations either need to be used with a substantially inflated uncertainty and/or with extreme caution. We have also only considered a single nonlinear term at a time; it may also be fruitful to consider mixtures or combinations of these nonlinearities, or a nonlinear term that accounts for the pattern effect by having a λ term that first increases and then correspondingly decreases. In any case, we have shown here that structural uncertainty plays an important role in reduced complexity climate models' total uncertainty, which must be accounted for in their physical projections, and especially in the socioeconomic projections that use such simple representations of climate physics.

Acknowledgments: We thank the many scientists whose collective work has generated the time series, prior information, and statistical method on which our work relies. We also thank Chris Smith for providing the radiative forcing time series ensemble as well as insightful comments. Cael acknowledges support from the National Environmental Research Council through Enhancing Climate Observations, Models and Data. GLB acknowledges support from the Simons Foundation. DAS acknowledges support from the Grantham Research Institute on Climate Change and the Environment at the London School of Economics, the ESRC Centre for Climate Change Economics and Policy (CCCEP; ref. ES/R009708/1), and the Natural Environment Research Council through Optimising the Design of Ensembles to Syupport Science and Society (ODESSS; ref NE/V011790/1)

References

[1] "Analyzing the dependence of global cloud feedback on the spatial pattern of sea surface temperature change with a Green's function approach". In: *Journal of Advances in Modeling Earth Systems* 9.5 (2017), pp. 2174–2189. DOI: https://doi.org/10.1002/2017MS001096. eprint: https://agupubs.onlinelibrary.wiley.com/doi/pdf/10.1002/2017MS001096. URL: https://agupubs.onlinelibrary.wiley.com/doi/abs/10.1002/2017MS001096.

[2] Timothy Andrews et al. "Accounting for Changing Temperature Patterns Increases Historical Estimates of Climate Sensitivity". In: *Geophysical Research Letters* 45.16 (2018), pp. 8490–8499. DOI: https://doi.org/10.1029/2018GL078887. eprint: https://agupubs.onlinelibrary.wiley.com/doi/pdf/10.1029/2018GL078887. URL: https://agupubs.onlinelibrary.wiley.com/doi/abs/10.1029/2018GL078887.

[3] Jonah Bloch-Johnson et al. "Climate sensitivity increases under higher CO2 levels due to feedback temperature dependence". In: *Geophysical Research Letters* 48.4 (2021), e2020GL089074.

[4] Raphael Calel and David A Stainforth. "On the physics of three integrated assessment models". In: *Bulletin of the American Meteorological Society* 98.6 (2017), pp. 1199–1216.

[5] Raphael Calel et al. "Temperature variability implies greater economic damages from climate change". In: *Nature communications* 11.1 (2020), pp. 1–5.

[6] Jule G Charney et al. *Carbon dioxide and climate: a scientific assessment*. 1979.

[7] Yue Dong et al. "Attributing Historical and Future Evolution of Radiative Feedbacks to Regional Warming Patterns using a Green's Function Approach: The Preeminence of the Western Pacific". In: *Journal of Climate* 32.17 (2019), pp. 5471–5491. DOI: 10.1175/JCLI-D-18-0843.1. URL: https://journals.ametsoc.org/view/journals/clim/32/17/jcli-d-18-0843.1.xml.

[8] Yue Dong et al. "Intermodel spread in the pattern effect and its contribution to climate sensitivity in CMIP5 and CMIP6 models". In: *Journal of Climate* 33.18 (2020), pp. 7755–7775.

[9] S. Fueglistaler. "Observational Evidence for Two Modes of Coupling Between Sea Surface Temperatures, Tropospheric Temperature Profile, and Shortwave Cloud Radiative Effect in the Tropics". In: *Geophysical Research Letters* 46.16 (2019), pp. 9890–9898. DOI: https://doi.org/10.1029/2019GL083990. eprint: https://agupubs.onlinelibrary.wiley.com/doi/pdf/10.1029/2019GL083990. URL: https://agupubs.onlinelibrary.wiley.com/doi/abs/10.1029/2019GL083990.

[10] Philip Goodwin and BB Cael. "Bayesian estimation of Earth's climate sensitivity and transient climate response from observational warming and heat content datasets". In: *Earth System Dynamics* 12.2 (2021), pp. 709–723.

[11] Jonathan M Gregory, Timothy Andrews, and Peter Good. "The inconstancy of the transient climate response parameter under increasing CO2". In: *Philosophical Transactions of the Royal Society A: Mathematical, Physical and Engineering Sciences* 373.2054 (2015), p. 20140417.

[12] Max Henrion and Baruch Fischhoff. "Assessing uncertainty in physical constants". In: *American Journal of Physics* 54.9 (1986), pp. 791–798.

[13] James Holte et al. "An Argo mixed layer climatology and database". In: *Geophysical Research Letters* 44.11 (2017), pp. 5618–5626.

[14] Chris Hope. "The $ 10 trillion value of better information about the transient climate response". In: *Philosophical Transactions of the Royal Society A: Mathematical, Physical and Engineering Sciences* 373.2054 (2015), p. 20140429.

[15] John J Kennedy et al. "An ensemble data set of sea surface temperature change from 1850: The Met Office Hadley Centre HadSST. 4.0. 0.0 data set". In: *Journal of Geophysical Research: Atmospheres* 124.14 (2019), pp. 7719–7763.

[16] Nicholas J Lutsko and Max Popp. "Probing the sources of uncertainty in transient warming on different timescales". In: *Geophysical Research Letters* 46.20 (2019), pp. 11367–11377.

[17] V. Masson-Delmotte et al. *Climate Change 2021: The Physical Science Basis. Contribution of Working Group I to the Sixth Assessment Report of the Intergovernmental Panel on Climate Change*. 2021.

[18] Colin P Morice et al. "An Updated Assessment of Near-Surface Temperature Change From 1850: The HadCRUT5 Data Set". In: *Journal of Geophysical Research: Atmospheres* 126.3 (2021), e2019JD032361.

[19] Zebedee RJ Nicholls et al. "Reduced Complexity Model Intercomparison Project Phase 1: introduction and evaluation of global-mean temperature response". In: *Geoscientific Model Development* 13.11 (2020), pp. 5175–5190.

[20] Matthew B Osman et al. "Globally resolved surface temperatures since the Last Glacial Maximum". In: (2021).

[21] Tim Rohrschneider, Bjorn Stevens, and Thorsten Mauritsen. "On simple representations of the climate response to external radiative forcing". In: *Climate Dynamics* 53.5 (2019), pp. 3131–3145. DOI: 10.1007/s00382-019-04686-4. URL: https://doi.org/10.1007/s00382-019-04686-4.

[22] SC Sherwood et al. "An assessment of Earth's climate sensitivity using multiple lines of evidence". In: *Reviews of Geophysics* 58.4 (2020), e2019RG000678.

[23] Christopher J Smith et al. "Energy budget constraints on the time history of aerosol forcing and climate sensitivity". In: *Journal of Geophysical Research: Atmospheres* 126.13 (2021), e2020JD033622.

[24] Kevin E Trenberth and Timothy J Hoar. "The 1990–1995 El Niño-Southern Oscillation event: Longest on record". In: *Geophysical research letters* 23.1 (1996), pp. 57–60.

[25] Laure Zanna et al. "Global reconstruction of historical ocean heat storage and transport". In: *Proceedings of the National Academy of Sciences* 116.4 (2019), pp. 1126–1131.

Climate nonlinearities: selection, uncertainty, projections, & damages
Supplementary material

B. B. Cael[1,*], G. L. Britten[2], F. Mir Calafat[1], J. Bloch-Johnson[3], D. Stainforth[4], & P. Goodwin[5]

1. National Oceanography Centre, Southampton, UK. 2. Massachusetts Institute of Technology, Cambridge, USA. 3. National Centre for Atmospheric Science, Reading, UK. 4. London School of Economics, UK. 5. University of Southampton, UK.

*cael@noc.ac.uk.

Extended Methods: We consider six energy balance models for the evolution of the global mean surface temperature anomaly T [°C] in response to the radiative forcing F [W/m^2] –

- $c\dot{T} = F - \lambda T$ (linear)
- $c\dot{T} = F - \lambda(1 + \lambda_T T)T$ (T-dependent feedback)
- $c\dot{T} = F - \lambda(1 + \lambda_F F)T$ (F-dep. feedback)
- $c(1 + c_T T)\dot{T} = F - \lambda T$ (T-dep. heat capacity)
- $c(1 + c_F F)\dot{T} = F - \lambda T$ (F-dep. heat capacity)
- $c\dot{T} = F - \lambda T - \lambda_s \int_{-\infty}^{0} \frac{1}{\tau} T(t') e^{t'/\tau}\ dt'$ (slow feedback)

where the dot represents a time derivative, c [J/m^{2}K] is the heat capacity of the Earth's surface layer represented by T, λ [W/m^{2}K] is the climate feedback parameter, $\lambda_{F,T}$ and $c_{F,T}$ are nonlinear terms corresponding to quadratic Taylor expansions of the linear model [3], and λ_s is a slow feedback term representing a multidecadal feedback on timescale τ [10]. By introducing a model selection parameter μ we can describe these in a single multimodel equation:

$$c(1 + \nu \mathbb{1}_{\mu=2} T + \nu \mathbb{1}_{\mu=3} F)\dot{T} = F + \lambda(1 + \nu \mathbb{1}_{\mu=4} T + \nu \mathbb{1}_{\mu=5} F)T + \mathbb{1}_{\mu=6} \lambda_s \int_{-\infty}^{0} \frac{1}{\tau} T(t') e^{t'/\tau}\ dt'$$

where ν represents the nonlinear terms in each case, $\mathbb{1}_X$ is an indicator function (i.e. equal to 1 if X is true and 0 otherwise), and μ takes on discrete values 1-6. The posterior mass function for μ will thus represent how much posterior probability corresponds to each of the six models.

We also investigated three slow (i.e. multidecadal) forcing-dependent models:

- $c\dot{T} = F - \lambda T - \frac{-\lambda_s}{\lambda + \lambda_s} \int_{-\infty}^{0} F(t') \frac{e^{t'/\tau}}{\tau}\ dt'$
- $c\dot{T} = F - \lambda T - \lambda_s T \int_{-\infty}^{0} \frac{1}{\tau} \frac{F(t')}{F(t)} e^{t'/\tau}\ dt'$
- $c\dot{T} = F - \lambda T - \lambda_s T \int_{-\infty}^{0} \frac{1}{\tau} \left(1 - \left|\frac{\dot{F}(t')}{F(t')}\right|\right) e^{t'/\tau}$

but all of these had negligible (< 0.01) posterior mass for μ when included, and were therefore not considered further. We also investigated a cubic model $c\dot{T} = F - \lambda(1 + \nu T(1 + \kappa T))T$ and found that there was a negligible difference in the posterior μ value for the cubic vs. quadratic (i.e. λ_T) model, but also that the cubic model's quadratic term ν was poorly constrained as was the sign of its cubic term $\nu \times \kappa$; the posterior essentially only specifies that the amplitude of the cubic term must be fairly small (Figure S8).

We evaluate equation 1 using the HadCRUT5 global mean surface temperature anomalies time series [18] and the radiative forcing time series provided in [17,23]. The latter is provided as an ensemble of estimates which is randomly sampled during the likelihood calculation process; F is thus an errors-in-variables term. T by contrast is given as a single value per year with an associated time-varying uncertainty σ. We leverage the prior information that there is a quasi-periodic fluctuation in the HadCRUT5 data due to climatic oscillations superimposed on the background climate state, most notably the El Nino Southern Oscillation with a dominant periodicity of $\leq$5 years [24], which does not correspond to the latent variable of interest here, that being the underlying global mean surface temperature anomaly. We therefore use a 5-year running mean of T and of σ, corresponding to the conservative assumption that all uncertainty in T is systematic. The choice of window size does not affect our conclusions (e.g. a 3-year or 7-year window yields nearly identical results). The modeled time-series are similarly smoothed to make them more comparable to the smoothed time series, as smoothing may have a small impact on long-term trends of interest, but whether or not this is done does not affect our conclusions.

Our prior choices for the parameters in Equation 1 above are as follows:

- μ is given a uniform prior over the numbers (1,2,3,4,5,6), giving no preference to any particular model.
- λ is given a log-normal prior of $lnN(0.78, 0.23)$. The choice of a log-normal parameterisation is because the log-normal distribution is its own inverse distribution, so choosing a log-normal prior for λ yields a log-normal prior for the climate sensitivity $S \propto \lambda^{-1}$, and vice versa; this therefore avoids some of the issues with implausibly heavy tails that arise in priors for S (λ) when choosing a prior for λ (S) [22]. The choice of parameter values is because λ represents both upward and downward fluxes of energy from the surface layer to which T corresponds. These upward fluxes were assigned a Gaussian prior $N(1.3, 0.44)$ by [22], while these downward fluxes were estimated to be $\sim$0.8$\pm$0.13 W/m^2 by Sherwood et al. [22]. The parameter values give a modal value of $\sim 2.1 \approx 1.3 + 0.8$ and a standard deviation of $\sim 0.46 \approx \sqrt{.44^2 + .13^2}$.
- c is given a Gaussian prior $N(9.67, 0.8)$ which is calculated from the number of seconds in a year (to make the HadCRUT5 timestep comparable to the units of the radiative forcing time series), the mean mixed layer depth (equally weighted in area and time) of the Argo mixed layer climatology [13], the density and heat capacity of seawater, and the sea surface temperature to global mean surface temperature warming ratio of HadSST4 [15] and HadCRUT5. We note that this prior is in good agreement with the c values estimated for the CMIP5 ensemble in [16] and that the uncertainty is dominated by uncertainty in which method is used to define the mixed layer depth.
- ν is given a Gaussian prior $N(0, 0.5)$ so as to be symmetric about zero (i.e. agnostic of the sign of the nonlinear term) and to assign a $\sim$95% prior probability that the nonlinear term is of a smaller amplitude than the linear term.
- λ_s is given a Gaussian prior $N(0.53, 0.23)$ following the analysis of CMIP5 and CMIP6 models in [8]. Note this leaves a small probability that λ_s is negative, as seen in some Earth system models.
- τ is given a log-normal prior $lnN(3.46, 0.23)$ because timescale uncertainty is typically relative rather than absolute, and these parameter values assign a $\sim$95% prior probability that τ is between 20-50 years and has a modal probability of 30 years [10].
- We also assign an uncertainty to the initial condition, i.e. the initial value of T in a time series, corresponding to the uncertainty in the first year of the HadCRUT5 time series.

The Bayesian inference procedure proceeds by sampling randomly from the above priors and the ensemble of F time series, using these to generate a model time series T_m and then evaluating the likelihood of that model T time series given the observational T time series and its uncertainty σ. Autocorrelation in the time series is accounted for by evaluating a multivariate Gaussian probability density function for the standardised errors $(T_m - T)/\sigma$ with a first order autoregressive covariance matrix. The posterior distributions are generated by sampling from the priors a billion times and weighing these prior probability samples by their relative likelihood. Posterior samples with negligible posterior probability are discarded for visualisations; >99.99% of posterior probability is retained. This version of importance sampling that we use is justified as there is good posterior-prior overlap. We verified that our results were stable and insensitive to prior assumptions respectively by repeating the analysis with new sets of random samples and by increasing or decreasing the priors' parameter values by 10%, both of which resulted in negligibly different posterior distributions.

From this posterior ensemble projections are made by forcing the time series with the SSP3-7.0 and SSP4-6.0 F time series from [17,23]. Damages are then calculated using the damage and discounting function script provided in [5], using the default parameters.

Paleo-likelihoods are derived from [22] for the LGM, mPWP, and PETM. The colder LGM temperature from [20] is also used for comparison. Likelihoods are evaluated by solving each of the six model equations at equilibrium ($\dot{T} = 0$). For the linear, $c_{F,T}$, and λ_s models, these can be evaluated analytically as the probability distribution of the quotient of two normal random variables; for the $\lambda_{F,T}$ cases these must be evaluated numerically by sampling many random T and F values from the corresponding Gaussian distributions for each paleoestimate, calculating their associated climate feedback value (which includes the effect of nonlinearity), and generating an empirical probability density function from these random samples. We consider the most recent cold period (the LGM), the most recent warm period (the mPWP), and the mPWP along with the warmest period on record (the PETM), as in [22]; we also consider the LGM with the newer temperature estimate from [20].

Supplementary Figures:

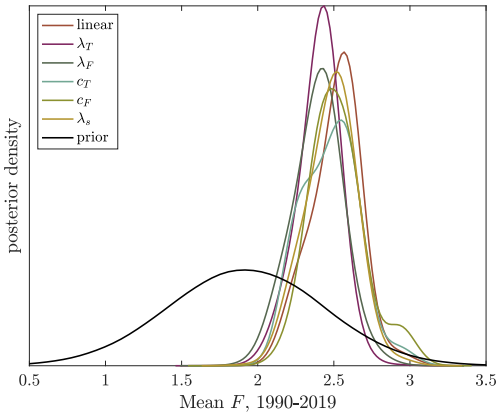

Figure S1. As Figure 1, but for the average of the radiative forcing from 1990-2020. The lower half of the radiative forcing estimates hold no posterior probability.

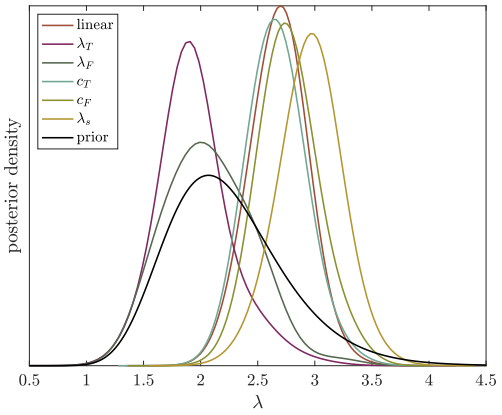

Figure S2. As Figure 1, but for λ. High λ values are favoured for models without temperature- or forcing-dependent feedbacks.

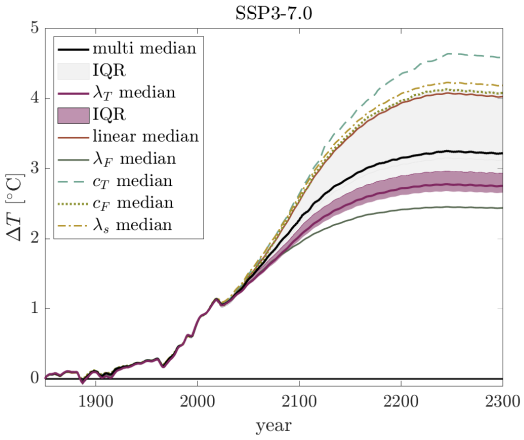

Figure S3. As Figure 2, but for SSP3-7.0. Structural uncertainty dominates parametric uncertainty, as for SSP4-6.0.

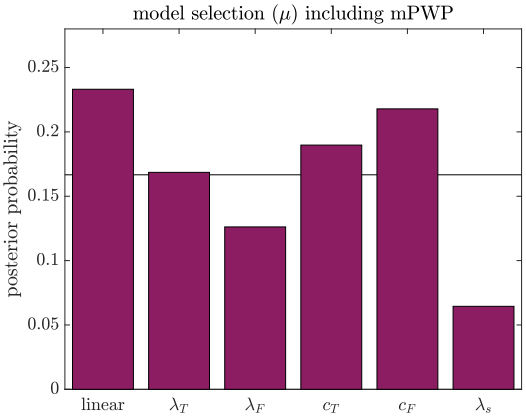

Figure S4. As Figure 1, but including a second likelihood function based on mid-Pleistocene warm period (mPWP) temperature and radiative forcing estimates.

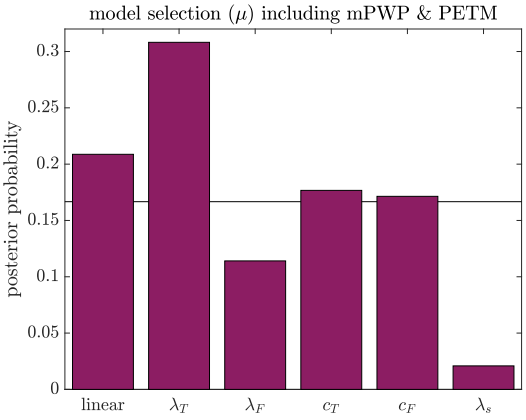

Figure S5. As Figure S4, but including a third likelihood function based on Paleocene-Eocene Thermal Maximum (PETM) temperature and radiative forcing estimates.

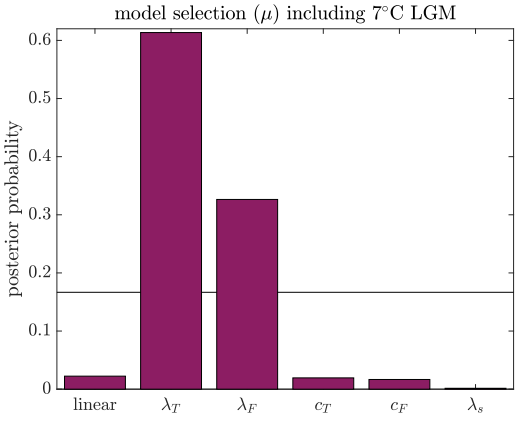

Figure S6. As Figure S4, but including a second likelihood function based on Last Glacial Maximum (LGM) temperature and radiative forcing estimates.

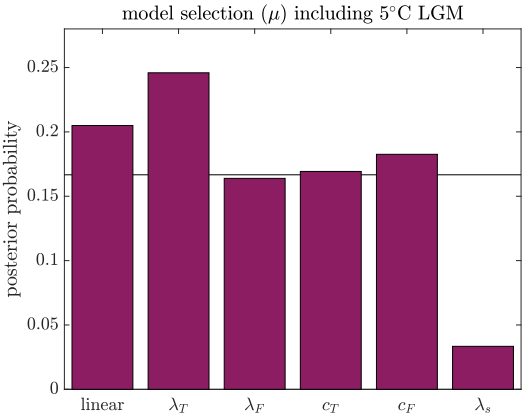

Figure S7. As Figure S6, but including the LGM temperature estimate from [20].

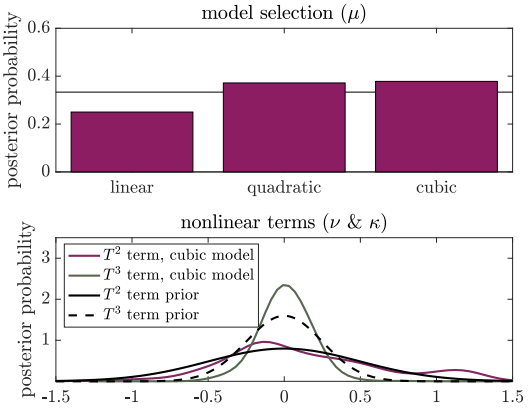

Figure S8. As Figure 1, but for the cubic case. The cubic and quadratic models have very similar posterior probability, but the posteriors for cubic term is symmetric about zero and has a lower standard deviation than its prior.